PERGAMON

International Journal of Multiphase Flow 28 (2002) 1–19

International Journal of Multiphase Flow

www.elsevier.com/locate/ijmulflow

Bubble behavior in subcooled flow boiling of water at low pressures and low flow rates

V. Prodanovic *, D. Fraser, M. Salcudean

Department of Mechanical Engineering, University of British Columbia, Vancouver, Canada

Received 1 September 2000; received in revised form 15 August 2001

Abstract

This study presents experimental data for subcooled flow boiling of water at pressures from 1.05 to 3 bar, bulk liquid velocities ranging from 0.08 to 0.8 m/s, and subcooling from 10 to 30 K. Experiments were carried out on a vertical, annular test section with inner heating surface and upward water flow. High-speed photography at rates of 6000–8000 frames/s captured bubble behavior from inception to collapse, bubble shapes during lifetime, detachment from the wall and typical bubble size. Bubble growth and condensation rates, and variation of bubble lifetime and size with flow rate, subcooling, heat flux and pressure were, further, examined and new correlations proposed.

Keywords: Subcooled flow boiling; Bubbles; Photographic study; Detachment

1. Introduction

Boiling occurs when the temperature of the heater surface exceeds the saturation temperature, thus causing bubble formation. If the bulk temperature of the liquid is below saturation, the process is known as subcooled boiling. Bubbles form in small pits and/or cavities on the heater surface filled with vapor. These vapor filled cavities are called nucleation sites. Bubble growth is affected by strong temperature and velocity gradients. It is widely accepted that typical bubbles slide along the surface of the heater, eventually detach from the surface and then condense rapidly when propelled into the cooler fluid core. Generally, their size and life span are strong functions of subcooling, surface superheat, flow rates and pressures, but also, functions of the cavity size, local surface temperature variations, influence of surrounding bubbles or local turbulence. All of these factors weave a complex interplay making the boiling process stochastic in nature. Understanding

* Corresponding author.
E-mail address: vladan@mech.ubc.ca (V. Prodanovic).

0301-9322/02/$ - see front matter
PII: S0301-9322(01)00058-1

bubble behavior during subcooled flow boiling is an important step in modelling void growth, bubble dynamics and boiling heat transfer.

The first photographic study of Gunther (1951) revealed the influence of liquid subcooling, heat flux and liquid velocity on bubble size, life span and population. Data were obtained for subcooled nucleate boiling of water on a vertical, electrically heated metal strip near burnout heat flux conditions. Bubbles were described as small hemispheres, growing and collapsing while sliding along the wall. Bubble size and lifetime decreased with increasing liquid velocity, subcooling and heat flux. Conversely, bubble population increased rapidly with increasing heat flux as burnout was approached. At higher subcooling bubbles did not detach from the surface of the heater, rather, they collapsed while attached to the wall.

Several researchers have focused on performing boiling experiments with water on a vertical annular test section: Frost and Kippenhan (1967) investigated bubble growth and bubble size during flow boiling of water that contained surfactants. Abdelmessih et al. (1972) used high-speed photography to observe the effect of liquid velocity on bubble growth and collapse from an artificial nucleation site. They concluded that the increase in liquid velocity resulted in a decreased bubble size and lifetimes whereas, an increase in heat flux had an opposite effect. The later was in contradiction with the results of Gunther (1951). Akiyama and Tachibana (1974) obtained bubble growth and collapse curves from experiments with water flowing upward through a vertical annulus with inner heater operating at atmospheric pressure. They presented data on the liquid temperature distribution normal to the heater surface. Del Valle and Kenning (1985) investigated the bubble size, life span and frequency as well as the interaction of nucleation sites at high heat fluxes. Their test section was an electrically heated stainless steel plate mounted on the side of a vertical, rectangular channel. In opposition to Gunther's experiments, they found that bubbles collapsed on their nucleation sites without sliding along the wall. They also commented on an inactivation of nucleation sites with increasing heat flux.

More recently Bibeau and Salcudean (1994) reported on the discrepancy between experimental investigations of bubble behavior, and void growth experiments with theoretical predictions at low pressures and liquid velocities. They conducted a bubble visualization study during subcooled boiling of water on the vertical, electrically heated annulus. Low flow velocities at atmospheric pressure were investigated. Their experiments revealed two types of bubble detachment: (1) parallel detachment, or detachment from the nucleation site that occurred almost immediately after inception and (2) normal detachment, or the point where bubbles detached perpendicular to the heater surface and subsequently collapsed in the cooler bulk fluid. They observed bubbles sliding and leaving the wall prior to collapse in all their experiments, including those close to ONB. Important observations were made on the shape of detaching bubbles and on the fact that detachment diameters were typically less than maximum diameters, showing that condensation started while bubbles were still attached to the wall. Similar observations were, also, reported by Zeitoun and Shoukri (1996) in a photographic study carried out with similar experimental setup.

Same observations on the two types of bubble detachment were presented by Klausner et al. (1993) who investigated vapor bubble departure of refrigerant R113 in saturated forced convection boiling from a horizontal, heating surface. Using the same experimental results, Zeng et al. (1993) further developed a model for prediction of both departure (parallel detachment) and lift-off (normal detachment) diameters.

Recently, Thorncroft et al. (1998) investigated bubble growth and detachment during vertical upflow and downflow boiling of a slightly subcooled FC-87. They reported that bubbles were typically sliding along the surface but remained attached to the wall in the upflow, in contrast to the downflow boiling where the lift-off was regularly occurring.

Tolubinsky and Kostanchuk (1970) investigated the flow boiling of water on a horizontal stainless steel plate with varying pressure. It was found that there was a strong dependence on bubble size with pressure, particularly for pressures between 1 and 5 bar. Other photographic studies of flow boiling on the horizontal surface include Koumoutsos et al. (1968) and, more recently Kandlikar and Stumm (1995), among others.

The present study investigated bubble behavior during subcooled flow boiling of water. Visual evidence was obtained with high-speed photography. The effects of liquid velocity, heat flux, subcooling and pressures on bubble dynamics were systematically investigated. Pressure ranged from 1 to 3 bar and hence, simulated the working conditions in low pressure pool-type SLOWPOKE and MAPLE nuclear reactors. This also represents the pressure range where the most dramatic changes in bubble size occur (Tolubinsky and Kostanchuk, 1970). The study is a continuation of void growth and bubble dynamics experiments carried out earlier by Bibeau and Salcudean (1994) using the same apparatus. Hence, altogether it provides a comprehensive database as a base for further void growth and bubble dynamics modelling.

2. Experimental apparatus

Shown in Fig. 1 is a schematic of the apparatus. The closed loop facility has a capacity of 3 m^3 and is fitted with a vertical, electrically heated, annular test section. Prior to entering the

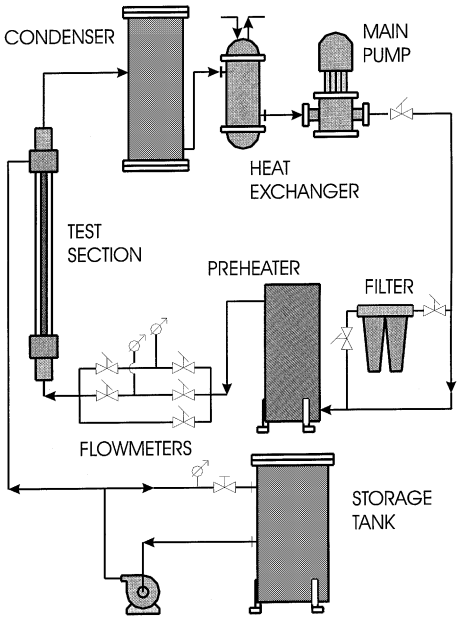

Fig. 1. The experimental apparatus.

test section the water is circulated from a storage reservoir through an immersion heater, filter and flow metering system. The liquid–vapor mixture exiting the test section passes through a condenser and heat exchanger before returning to the reservoir. The loop allows for varying pressure, flow rate and inlet temperatures of the liquid. Thus, one can obtain a desired subcooling at the filming location along the test section. The test section is 0.78 m long and consists of an electrically heated rod and an outer quartz glass tube (22 mm ID). The heater is a 12.7 mm diameter hollow stainless steel rod welded to solid copper rods. The heated length of 0.48 m is located 0.22 m downstream of the inlet plenum thus allowing for the flow to fully develop. A large range of heat fluxes was supplied to the test section with the 64 kVA power supply.

Temperatures at the wall, inlet and outlet of the test section, were measured with *K*-type thermocouples. An intrinsic thermocouple with leads embedded in the surface at the filming location (0.44 m downstream of the start of heated section) was used for wall temperature measurements. Isolation modules were used to isolate the signal from the electrical heating from that developed by the thermocouple.

Inlet and outlet static pressures were measured with bourdon type gauges. The volumetric flow rate was measured with two turbine flow meters that cover a range of 0.006–0.6 l/s. Conditioned signals were fed to a high-speed analog/digital I/O expansion board (Metrabyte DAS20) and processed using LABTECH NOTEBOOK software. The estimated errors for measured parameters are shown in Table 1.

Bubbles were filmed with a 16 mm High Speed Motion Picture Camera HYCAM K20S4 E fitted with MACRO lens and KODAK Eastman Ektachrome H-S 7250 films. Allowable film speeds were between 4000 and 8000 frames/s. The camera was located around 0.44 m from the start of the heated section and could capture a region of about 8 mm along the heater surface. A single film could capture about 1s of the boiling process. Time steps of 1ms were marked on the film using a 1 kHz pulse generator. Films were digitized using a CCD camera (TAMRON/FOTOVIX II). These were later studied using image analysis software. Each digitized image was enlarged 100 times to allow accurate measurements of the bubble geometry. A square cross-sectional glass box filled with water surrounded the test section to correct distortion due to refraction. Lighting consisted of eleven 300 W halogen projector lamps. A ground glass screen served to diffuse the light source. The test section details and photographic setup are shown in Fig. 2.

Table 1
Estimated errors for experimental parameters

Measured parameters	Error (+/−)
Pressure	140 Pa
Temperature	1.0 K
Volumetric flow rate	0.3%
Heat flux	2%
Time	0.02 ms
Bubble diameter	0.05 mm

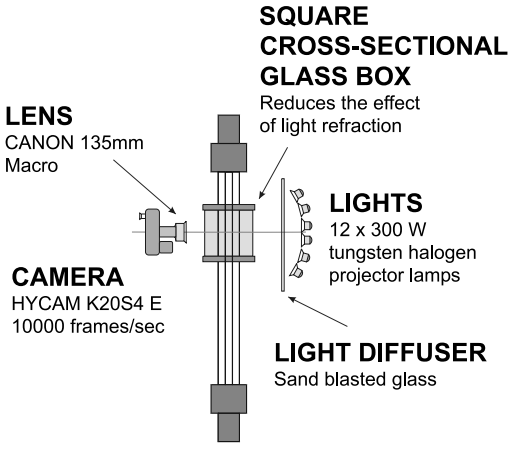

Fig. 2. The test section and photographic setup.

3. Image analysis

The present study is based on 61 films taken at pressures of 2 and 3 bar (29 at 2 = bar and 32 at 3 bar). As well, 45 previous films for 1 bar taken by Bibeau and Salcudean (1994) were also included in the analysis. Their data were obtained on the same apparatus. The mass flow rates ranged from 0.02 to 0.2 kg/s, corresponding to mean liquid velocities, U_b, from 0.08 to 0.8 m/s in the annular test section. Inlet temperatures were adjusted to obtain desired subcooling, ΔT_{sub} (10, 20 and 30 K) at the filming location.

The heat flux, ϕ, was varied systematically from 0.2 to 1 MW/m^2 while, for each test, local subcooling and flow rate, were held constant. Such a range covers the boiling process from the appearance of the first bubble, commonly known as the onset of nucleate boiling (ONB), to the higher heat fluxes beyond the onset of significant void (OSV). The OSV denotes the location where the void growth curve takes much steeper path resulting in significant increase in the amount of vapor. The model of Hahne et al. (1990), was used to calculate the heat flux at ONB. The heat flux at OSV was obtained from a correlation by Bibeau and Salcudean (1993). It is a modification of Saha and Zuber's model to account for the liquid velocity (i.e., variation of the Nusselt number at OSV).

Approximately 100 bubbles from each film were used to obtain detachment diameters and 10–30 bubbles were analyzed from inception to collapse. The arithmetic mean was used as a typical detachment diameter for each given set of experimental conditions. Upon analyzing bubbles from inception to collapse, a significant difference in bubble diameters and lifetimes for bubbles on the same film (same experimental conditions) has been observed. This has been attributed to the fact that bubbles: (1) were initiated from different nucleation sites and/or (2) experienced varying local temporal thermal and velocity fields. The authors' view was that the later effects are dominant in creating scatter in experimental data. Fig. 3 shows the bubble size and lifetime distribution from different nucleation sites at fixed conditions. It was, therefore, necessary to establish a mechanism for identifying typical bubbles from each film. Typical bubbles in this study are those, whose lifetimes, detachment diameters and initial growth rates are closest to averages for a given set of experimental conditions.

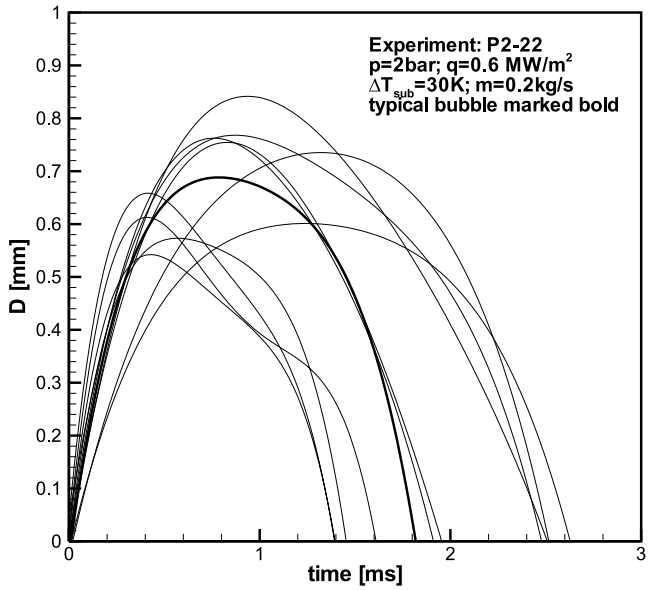

Fig. 3. Bubbles initiated from different nucleation sites on the same film.

The mean diameters, D, were calculated from measurements of 32 different Feret diameters (distances between opposing parallel tangents on the surface of the bubble – i.e., close to the bubble diameter). Also, the maximum and minimum Feret diameters were taken to represent two diameters along principal axes of the bubble (typically normal and parallel to the surface of the heater). Thus, their ratio represents the elongation of the bubble.

A projection of the bubble centroid on the surface of the heater on the first frame was assumed to be the location of the nucleation site. Distances from the nucleation site to the location of the bubble centroid on each subsequent frame showed the displacement of the bubble in the directions normal and parallel to the heater. These geometrical parameters are shown in Fig. 4(a). Bubble growth time, t_m, condensation time, t_c, and lifetime, t_b, were deduced from the mean diameter, D, vs. time graphs, as shown in Fig. 4(b). A list of typical bubbles from experiments in the "isolated bubble region" (as explained below) is given in Table 2.

4. Results and discussion

4.1. Qualitative analysis of bubble behavior

The experiments have shown that bubble behavior within the given range of flow rates and heat fluxes, cannot be represented by a single model. This is despite the fact that most of the bubbles within the region bounded by the ONB and OSV behaved in a similar manner, as described below. Immediately after inception, typical bubbles detached from their nucleation site and started sliding. This is referred to as parallel detachment (Bibeau, 1993) or bubble departure (Klausner). The explosive bubble growth rate at the early stages was reduced in time. Bubbles, after reaching

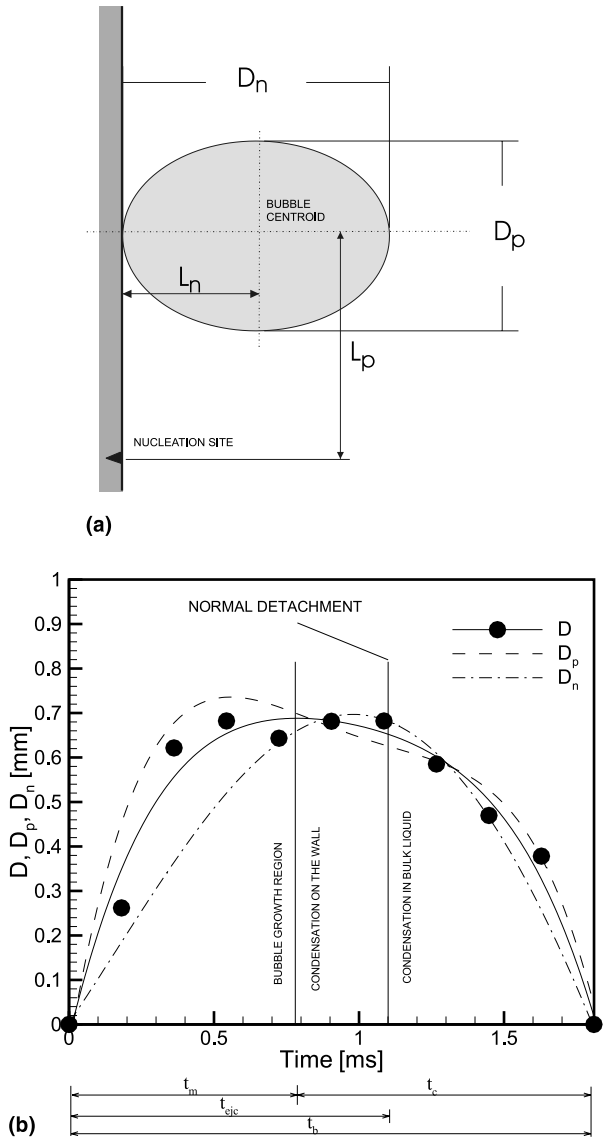

Fig. 4. (a) The measured geometrical parameters. (b) Typical bubble for experiment P2-22.

their maximum diameters, generally began shrinking while still attached to the surface of the heater. After sliding a certain distance bubbles typically detached from the surface and were propelled into the fluid core, where they collapsed. This point is known as the normal detachment (Bibeau) or bubble lift-off (Klausner).

For the present study normal detachment was not observed at low heat fluxes, close to ONB. Although bubbles were occasionally seen to detach from the heater, one cannot adopt this as typical bubble behavior. Also, at high heat fluxes, close to OSV, the significant interaction between bubbles has led to the conclusion that the bubble detachment mechanism differed from

Table 2

Label	U_b (m/s)	ϕ (MW/m^2)	ΔT_{sub} (K)	D_m (mm)	D_{ejc} (mm)	t_b (ms)	t_{ejc} (ms)	Lp_{ejc} (mm)
(a) *Typical bubbles* $p = 1.05$ *bar*								
P1-05	0.42	0.30	30	1.52	1.33	5.09	3.72	1.34
P1-06	0.83	0.50	30	1.26	1.08	2.91	2.24	1.63
P1-12	0.83	0.60	30	1.58	1.18	5.11	4.28	3.49
P1-13	0.83	0.80	30	1.14	0.94	2.56	1.76	1.29
P1-14	0.83	0.90	30	0.89	0.81	2.22	1.59	1.40
P1-16	0.42	0.60	30	1.28	0.93	2.41	1.93	1.08
P1-17	0.42	0.80	30	0.99	0.80	2.35	1.99	1.00
P1-18	0.42	0.90	30	0.87	0.80	1.79	1.39	0.48
P1-21	0.84	0.60	20	1.45	1.24	4.11	2.15	2.25
P1-22	0.84	0.70	20	1.24	1.06	3.92	2.55	2.11
P1-24	0.42	0.30	20	2.67	2.19	9.94	6.70	2.62
P1-25	0.42	0.60	20	1.64	1.53	5.39	3.85	1.94
P1-26	0.42	0.70	20	1.31	1.25	4.50	2.37	1.78
P1-27	0.08	0.20	20	2.86	2.18	10.87	6.90	2.13
P1-28	0.08	0.30	20	3.24	2.68	13.24	9.50	−0.63
P1-33	0.42	0.30	10	2.18	1.98	9.53	6.23	2.48
P1-34	0.08	0.10	10	1.93	1.85	18.61	6.86	0.98
P1-35	0.08	0.20	10	2.57	2.48	14.67	8.31	2.05
P1-36	0.08	0.30	10	2.09	1.82	9.57	6.05	0.23
P1-37	0.08	0.20	30	1.57	1.14	3.30	2.68	0.22
P1-39	0.83	0.60	40	1.23	0.77	2.14	1.75	1.21
P1-40	0.83	0.90	40	1.21	0.59	2.10	2.10	1.23
P1-41	0.83	1.20	40	0.92	0.75	1.55	1.35	1.05
P1-42	0.82	0.60	60	0.94	0.66	1.43	1.23	0.80
P1-44	0.82	1.20	60	0.90	0.68	1.53	1.27	0.56
(b) *Typical bubbles* $p = 2$ *bar*								
P2-02	0.41	0.4	20	0.5645	0.5361	1.728	0.96	0.2258
P2-03	0.41	1	30	0.8429	0.6769	1.827	1.218	0.320302
P2-04	0.41	0.8	30	0.8565	0.6741	2.064	1.204	0.32547
P2-05	0.41	0.6	30	0.7498	0.7193	2.502	1.39	0.269928
P2-06	0.41	0.4	30	0.9891	0.9234	3.19	1.595	0.405531
P2-10	0.08	0.4	20	0.8274	0.7569	3	1.5	0.099288
P2-20	0.82	0.4	20	0.7139	0.6517	2.592	1.44	0.656788
P2-08	0.41	0.6	20	0.7848	0.7121	2.38	1.19	0.298224
P2-09	0.82	0.6	20	0.7122	0.6306	1.862	0.931	0.334734
P2-11	0.41	0.32	10	0.7343	0.7343	3.145	1.11	0.044058
P2-18	0.82	0.36	10	0.7921	0.7791	3.64	1.43	0.570312
P2-22	0.82	0.6	30	0.6822	0.6821	1.81	1.086	0.586692
P2-23	0.82	0.8	30	0.5968	0.5784	1.379	0.788	0.364048
P2-15	0.08	0.2	30	0.7907	0.7907	2.214	0.984	0.102791
(c) *Typical bubbles* $p = 3$ *bar*								
P3-41	0.82	0.6	29.9	0.4708	0.4315	2.379	1.281	0.724999
P3-42	0.82	0.8	29.6	0.4231	0.4033	1.65	1.05	0.315
P3-43	0.82	1	29.5	0.4693	0.4512	1.665	0.925	0.706
P3-47	0.41	0.6	29.4	0.486	0.47	1.538	0.577	0.0980019
P3-48	0.41	0.8	30.4	0.3722	0.3662	0.828	0.414	0.1680111

Table 2 (*continued*)

Label	U_b (m/s)	ϕ (MW/m^2)	ΔT_{sub} (K)	D_m (mm)	D_{ejc} (mm)	t_b (ms)	t_{ejc} (ms)	Lp_{ejc} (mm)
P3-49	0.41	1	31.7	0.3779	0.3077	0.815	0.489	0.1519914
P3-27	0.08	0.2	28.7	0.528	0.528	2.104	1.052	0.2139614
P3-52	0.08	0.3	31	0.6043	0.6043	4	1	0.0030215
P3-37	0.82	0.6	20.2	0.516	0.4109	2.352	1.617	1.0204055
P3-39	0.82	0.8	19.1	0.5119	0.5119	3.178	1.135	0.6963017
P3-29	0.41	0.4	18.9	0.439	0.439	2.208	0.92	−0.070064
P3-24	0.41	0.6	22.5	0.388	0.363	1.27	0.762	0.0529581
P3-26	0.08	0.2	19.8	0.579	0.55	4.284	1.53	0.2521719
P3-51	0.08	0.3	20.8	0.5508	0.5064	4.446	0.936	0.2095243
P3-45	0.41	0.3	13.5	0.533	0.533	2.387	1.023	0.4106019

those seen at lower heat fluxes. From these observations, one can divide the boiling process between ONB and OSV into three regions as follows:

4.1.1. The low heat flux region

The observed bubble population in this region was relatively low (about 3–8 bubbles per 1 cm of length of the heater). Bubbles were roughly spherical and did not change significantly in size and shape. They were all observed to slide along the heater. Detachments were rarely observed and were usually preceded by some disturbance, like merging or touching between two bubbles. The authors conclude that detachments were caused by sudden change in size and/or shape of bubbles.

Also typical for this region was that most of the detached bubbles remained close to the wall, eventually reattaching a few frames later. Very few actually collapsed in the bulk fluid. Bubble reattachment in the low heat flux region was not, to the author's best knowledge, previously reported in the open literature except in the flow boiling review by Butterworth and Shock (1982). According to this review, Mori has performed experiments on bubble growth on a vertical wall in saturated boiling at zero gravity, and noticed that, at low superheat, bubbles would detach and reattach. No detailed discussion on this phenomenon was found. Although probably insignificant relative to the overall heat transfer, a closer look at the reattachment could possibly help to understand the origin of bubble detachment. During these experiments bubble reattachment was seen regularly and can be adopted as typical low heat flux bubble behavior.

Bubble behavior close to ONB was previously discussed (e.g., Bibeau and Salcudean, 1994). Their first conclusion was that bubbles did not detach. This was later corrected by closer examination of larger area of the heater. No comments on the nature and mechanism of these detachments were offered.

4.1.2. The isolated bubble region

The term was "borrowed" from pool boiling terminology. It accurately describes observations at moderate heat fluxes and denotes the region in which bubbles are growing, detaching and collapsing without significant influence from neighboring bubbles. Bubbles slid about a couple diameters or less before being propelled into the fluid core. The sliding of bubbles was likely attributable to both, drag and buoyancy. The experiments showed that large bubbles growing

under low liquid velocity and low heat flux conditions, slid at speeds higher than the bulk liquid velocity (i.e., slip ratio >1.0). This is likely due to buoyancy effects. As the size of bubbles decreased the sliding velocity dropped below the bulk liquid velocity with the slip ratio of about 0.8 for high heat flux, high subcooling experiments.

Bubbles were seen to extend significantly into the bulk fluid where they collapsed rapidly. The speed at which bubbles were propelled into the bulk liquid varied with heat flux and local subcooling. Higher heat fluxes and subcooling (which produced higher temperature gradients) affected bubble motion in the direction normal to the wall by increasing their speed. Also, bubbles exposed to higher temperature gradients were seen to collapse closer to the wall. However, the location of bubble collapse measured from the wall and "normalized" with maximum diameter did not show a significant variation with heat flux. Instead, it remained relatively constant throughout the experiments.

Overall, bubbles in this region were not spherical. Upon inception, bubbles were generally flattened, likely due to strong inertial forces. As they grew while sliding on the surface, they became more rounded, having a spherical shape near the maximum diameter. After reaching their maximum size, they typically continued to slide while shrinking and becoming more elongated. The observed ratio $F = D_p/D_n$, representing the elongation of bubbles at normal detachment from these experiments was between 0.8 and 0.85. These values are in agreement with previous qualitative observations of the shape of bubbles (Akiyama and Tachibana, 1974; Bibeau and Salcudean, 1994, Faraji et al., 1994). They reported that this ratio was typically around 0.8 for experiments taken at 1.05 bar.

4.1.3. Significant bubble coalescence region

As the heat flux was raised, approaching OSV, bubble population increased significantly. Many merged before detachment, thus creating larger bubbles. Smaller, isolated bubbles still exhibited the behavior described above. They were significant in number, usually growing in the wake of the larger bubbles. It was observed that various factors triggered bubble detachment. Aside from a typical normal detachment, many bubbles detached after merging or interacting with neighboring bubbles. Detachments also occurred when a new bubble, growing underneath a passing bubble, apparently pushed the one on top away. Due to large bubble populations, significant coalescence was observed after detachment thus forming larger bubbles. These large bubbles kept sliding or travelling close to the surface of the heater and further coalesced.

It should be emphasized that the above three boiling regions were observed for all fixed subcooling and flow rate. Thus, they depend on the heat flux. However, this last region (significant bubble coalescence) was not observed at $p = 1.05$ bar (Bibeau and Salcudean, 1994) and only partially at $p = 2$ bar. It becomes obvious for the $p = 3$ bar experiments due to increasing number of active nucleation sites with increasing pressure.

It is also not clear, at this point, if the transition between the "low heat flux region" and the "isolated bubble region" can be related to the transition from the commonly referred partial nucleate boiling to fully developed nucleate boiling. Observations of different bubble behavior lead to the conclusion that the heat transfer mechanism in the two regions would be different. While in the low heat flux region the latent heat transport through sliding bubbles can be considered the main heat transfer mode, in the isolated bubble region bubble agitation may be dominant. With the increase in bubble population, the overall heat transfer would increase due to

at least two coupled effects: increased bubble agitation and increased latent heat transport. Also, the increase of void past OSV would affect the convective heat transfer (macroconvection) by accelerating the liquid phase. This was partly discussed in Bibeau and Salcudean (1994). A thorough heat transfer analysis is beyond the scope of this study. Shown in Fig. 5 are typical photographs of all three above mentioned regions.

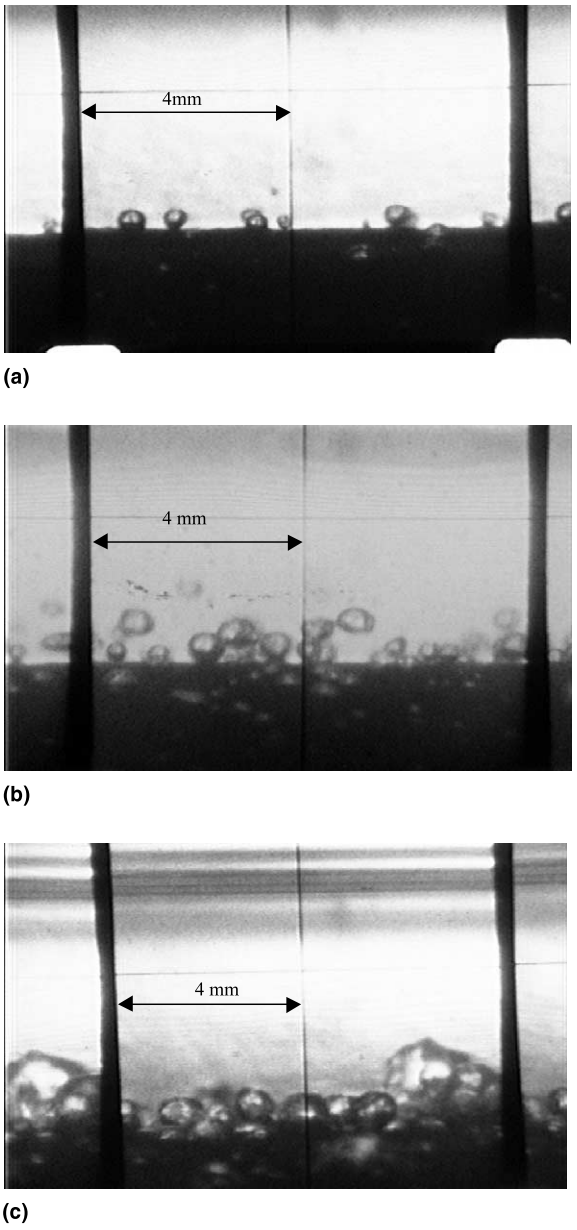

Fig. 5. (a) Bubble behavior in the low heat flux region. (b) Bubble behavior in the isolated bubble region. (c) Bubble behavior in the significant coalescence region.

Bubble sizes and lifetimes are predominantly affected by heat flux, subcooling, bulk liquid velocity and pressure. An attempt was made in the present study to isolate and observe the effect of each of these parameters. The following is a qualitative discussion of the observed trends.

Bubble size decreases with increased subcooling at fixed flow rates and heat fluxes. Lower temperature gradients in the liquid surrounding a bubble reduce the condensation rates, thus allowing larger diameters. This is in agreement with most of the previous experimental studies (e.g., Gunther, 1951; Zeitoun and Shoukri, 1996; Tolubinsky and Kostanchuk, 1970; Faraji et al., 1994; Roy et al., 1994; Kandlikar et al., 1995). Bubble lifetimes and ejection times also tend to decrease with increased subcooling.

Various opinions can be found in the literature on the effect of heat flux on maximum bubble diameters. Gunther (1951) has concluded that bubble size decreases with increasing heat flux, Tolubinsky and Kostanchuk (1970) reported no effect of heat flux on bubble dimensions while Abdelmessih et al. (1972) observed larger bubbles and longer lifetimes with an increase in heat flux. From the present study it can be concluded that generally bubble maximum diameters drop with increasing heat flux with constant flow rates and subcooling. This is particularly evident at lower heat fluxes while at higher heat flux bubble diameters remained roughly constant. These findings are in agreement with the previous investigation (Bibeau and Salcudean, 1994).

Bubble lifetimes and ejection times also depend on heat flux. They show similar behavior as bubble maximum diameters, with the reduction of bubble life span being more evident with increasing heat flux closer to ONB. These trends have been observed within the whole pressure range.

The effect of the liquid velocity on bubble sizes and lifetimes was, again, more pronounced at lower heat flux. Bubble diameters and lifetimes decreased with increasing flow rates. This became less pronounced as the OSV was approached.

Bubble diameters appear to be strongly dependent on pressure. Experimental results from this study agree with the observations of Tolubinsky and Kostanchuk (1970) (i.e., maximum diameters decrease with increasing pressure). However, from the present study one cannot confirm their findings that increasing pressure results in an increase of the contact time between the bubble and the surface (i.e., longer ejection time). On the contrary, both, bubble lifetimes and ejection times, as well as their ratio, t_{ejc}/t_b, tend to decrease with increasing pressure. Fig. 6 represents an illustration of the change in bubble size and lifetimes with pressure as well as with heat flux. All bubbles in Fig. 6 originate from the experiments with same mass flow rate ($m = 0.1$ kg/s) and subcooling ($\Delta T_{sub} = 30$ K).

As mentioned above, during growth bubbles transform from a flattened to an elongated shape. This behavior was observed at all pressures, subcoolings and flow rates, in agreement with the previous observations (Bibeau and Salcudean, 1994; Zeitoun and Shoukri, 1996). Bubble detachment diameters are smaller than maximum diameters indicating that condensation rates overcome evaporation rates while bubbles are still attached to the surface of the heater. The maximum elongation of bubbles is reached right before detachment.

Bubble population increases with decreasing flow rate. This is particularly evident at lower heat fluxes where the single-phase forced convection still plays an important role. At lower flow rates one expects lower convection heat flux coefficients causing higher local surface temperatures and increasing the number of active nucleation sites. Bubble population also increases with increasing heat flux. At high heat flux, close to OSV, large bubbles, formed as a result of significant coalescence, affect the overall bubble behavior.

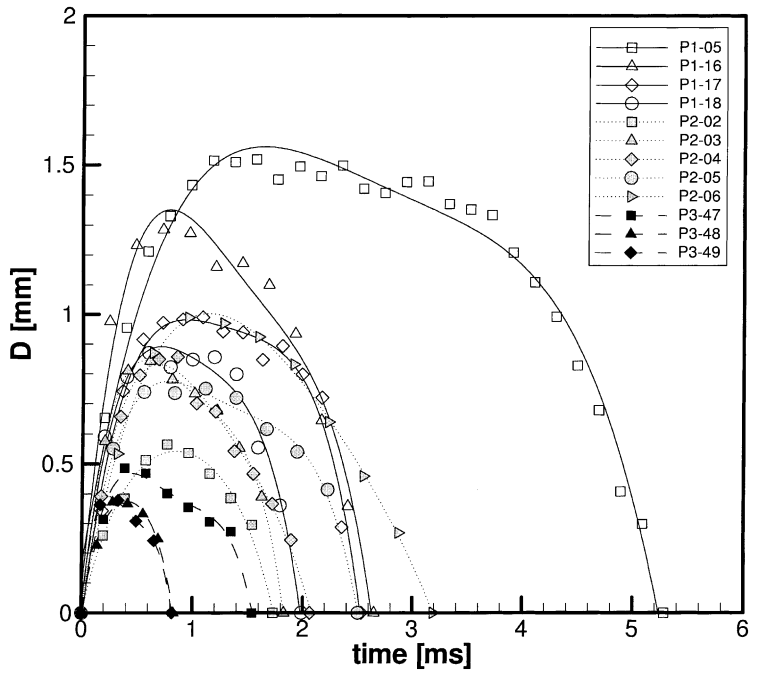

Fig. 6. Variation of bubble size and lifetime with pressure and heat flux at constant mass flow rate ($m = 0.1$ kg/s) and subcooling ($\Delta T_{sub} = 30$ K).

5. Correlation of experimental data

To correlate bubble growth and condensation rates in terms of maximum bubble radius and bubble lifetime, the equation for normalized bubble diameters in the form suggested by Akiyama and Tachibana (1974) was adopted. The correlation is given by Eq. (1)

$$\frac{D}{D_m} = 1 - 2^K \left| \frac{1}{2} - \left(\frac{t}{t_b} \right)^N \right|^K, \tag{1}$$

where N and K are the empirical constants shown in Table 3. Predictions obtained with Eq. (1) and the current data are shown in Fig. 7.

Despite its importance in analyzing the interfacial area concentration and void growth modelling, a substantial deficit of bubble detachment diameter correlations exists in the open literature for the flow boiling conditions as compared to pool boiling. Also, many researchers equate the maximum and detachment diameters thus not taking into account that bubbles in subcooled flow boiling start condensing while still attached to the wall.

Zuber (1961) developed a model based on the assumption that the heat transfer through the vapor–liquid interface controls bubble growth. The model is based on the Bosnjakovic equation, originally developed for bubble growth in a stagnant, superheated liquid with uniform temperature. Zuber's modification accounted for the existence of a non-uniform temperature field.

Table 3
Bubble growth and condensation correlations

Experiment	N	K
Akiyama and Tachibana	$0.25 < t_m/t_b < 0.5$ Calculated for given range using $D/D_m = 1$ when $t/t_m = 1$	3
Bankoff (Gunther's data)	$0.32 < t_m/t_b < 0.57$ Calculated for given range using $D/D_m = 1$ when $t/t_m = 1$	2
Faraji et al.	$t_m/t_b = 0.33; N = 0.67$	2.2
Present Study	$t_m/t_b = 0.37; N = 0.7$	2.5

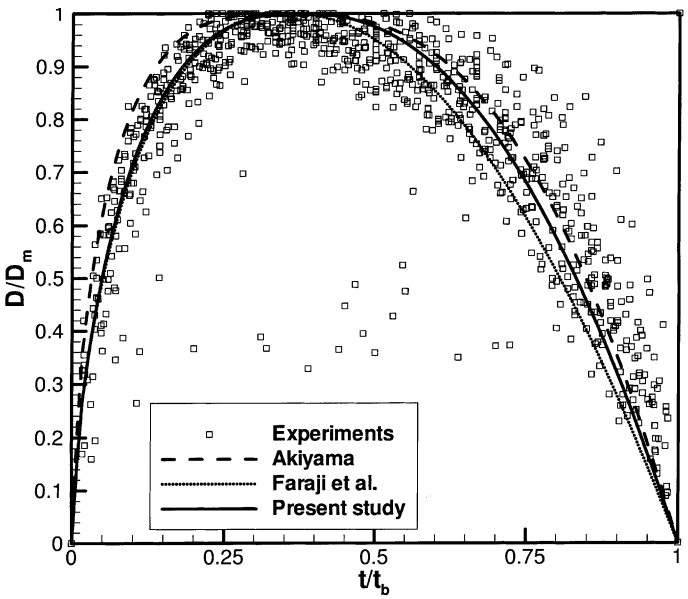

Fig. 7. Correlations for bubble growth and condensation rates.

Another model that falls into the same category regarding the dominant heat transfer mode is that of Mikic et al. (1970).

Unal (1976) has used the microlayer evaporation concept to develop a model for maximum bubble diameters and bubble growth times. The heat is supplied to the bubble through a thin liquid microlayer separating the bubble from the solid surface. This model does not take into account the condensation effects.

Serizawa (1979) introduced a concept of bubble boundary layer. According to this approach, bubbles detach from their nucleation sites but stay close to the surface thus creating a bubble layer adjacent to the surface. He suggested an empirical model for predicting bubble detachment diameters.

Faraji et al. (1994) presented correlations for maximum bubble diameter, bubble lifetime and condensation time in terms of Jakob number and dimensionless subcooling. They did not

explicitly include pressure variations in their model. Their correlations are limited to $p = 1$ bar.

Zeitoun and Shoukri (1996) presented a correlation for the Sauter diameter using a relatively complex function of *Re*, *Ja*, *Bo* and density ratio ρ_l/ρ_v. A comparison of current data with these correlations is shown in Fig. 8.

Zuber (1961) and Mikic et al. (1970) significantly over-predict the maximum diameters. The concept of evaporation at the vapor–liquid interface does not seem to be appropriate for the experiments presented in this study. In fact, the microlayer concept (Unal, 1976) leads to acceptable predictions for maximum bubble diameters over the whole range of pressures. The model of Zeitoun and Shoukri (1996) slightly under-predicts the detachment diameters at $p = 1$ bar but over-predicts experimental data at higher pressures. Serizawa (1979) consistently under-predicts the experimental data.

Following the suggestion by Cooper et al. (1983) for the non-dimensional maximum bubble radius and applying similar procedures for the non-dimensional bubble lifetime as in Faraji et al. (1994), several correlations, covering pressures up to 3 bars were developed. The non-dimensional maximum and detachment diameters D_m^+, D_{ejc}^+, maximum bubble diameter time, t_m^+, bubble ejection time, t_{ejc}^+, and bubble condensation time t_c^+, are given by Eqs. (2) and (3).

$$D_m^+ = \frac{D_m \sigma}{\rho_l \alpha_l^2}, \quad D_{ejc}^+ = \frac{D_{ejc} \sigma}{\rho_l \alpha_l^2}, \tag{2}$$

$$t_m^+ = \frac{t_m \alpha_l}{\left(\frac{\rho_l \alpha_l^2}{\sigma}\right)^2}, \quad t_{ejc}^+ = \frac{t_{ejc} \alpha_l}{\left(\frac{\rho_l \alpha_l^2}{\sigma}\right)^2}, \quad t_c^+ = \frac{t_c \alpha_l}{\left(\frac{\rho_l \alpha_l^2}{\sigma}\right)^2}. \tag{3}$$

The symbol α_l represents the thermal conductivity and σ is the surface tension. The experimental data were correlated with four parameters, Jakob number, *Ja*, non-dimensional subcooling, θ, Boiling number, *Bo*, and density ratio, ρ_l/ρ_g. These dimensionless parameters account for all

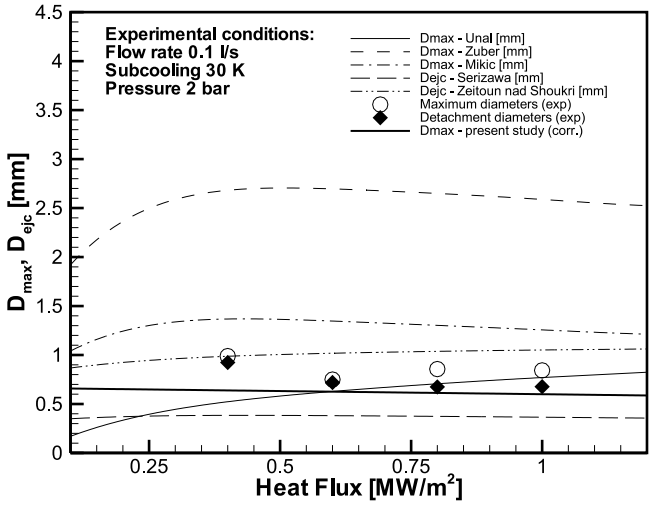

Fig. 8. Comparison of bubble diameter models with experimental data.

Table 4
Correlation coefficients

Variable	A	b	c	d	e
D_m^+	236.749	−0.581	−0.8843	1.772	0.138
D_{ejc}^+	440.98	−0.708	−1.112	1.747	0.124
t_m^+	9.625e8	−1.362	−1.977	2.102	0.142
t_{ejc}^+	1.522e9	−1.681	−2.182	2.459	0.262
t_c^+	1.138e8	−1.197	−1.686	2.389	0.169

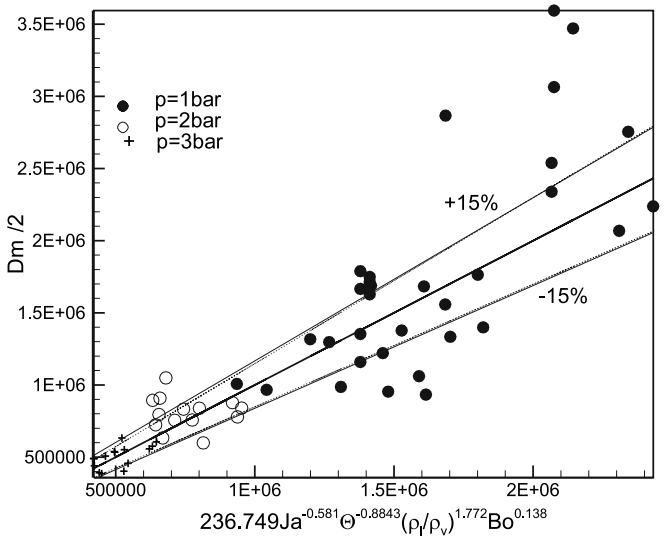

Fig. 9. Correlation for the normalized maximum bubble diameter.

relevant variables affecting bubble diameters and lifetimes. The definitions of Ja, θ, and Bo are given by Eqs. (4)–(6). The ratio ρ_l/ρ_v was found to represent well the influence of the pressure on bubble behavior.

$$Ja = \frac{\rho_l c p_l (T_w - T_{sat})}{\rho_v i_{fg}}, \tag{4}$$

$$\theta = \frac{T_w - T_b}{T_w - T_{sat}}, \tag{5}$$

$$Bo = \frac{\phi}{G i_{fg}}. \tag{6}$$

The symbols T_w, T_b and T_{sat} represent the wall temperature, bulk liquid temperature and saturation temperature, respectively. The variable G is the mass flux. The correlation in the form shown in Eq. (7) was proven to give satisfactory results

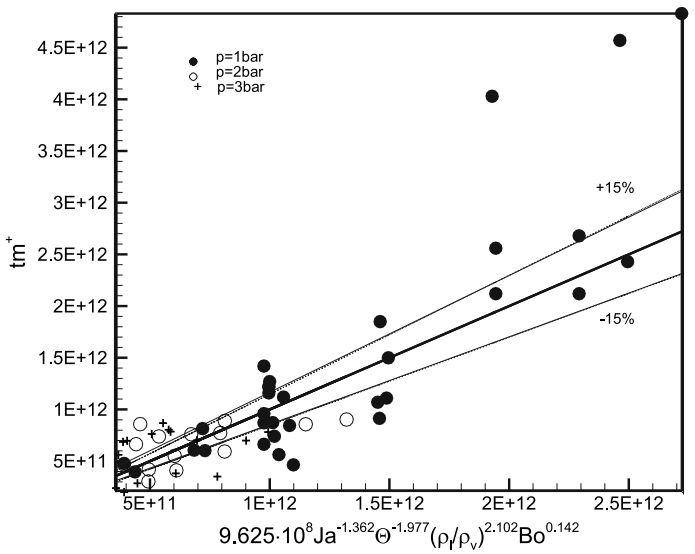

Fig. 10. Correlation for the normalized bubble growth time.

$$D_{\mathrm{m}}^{+}, D_{\mathrm{ejc}}^{+}, t_{\mathrm{m}}^{+}, t_{\mathrm{ejc}}^{+}, t_{\mathrm{c}}^{+} = AJa^{b}\theta^{c}\left(\frac{\rho_{1}}{\rho_{v}}\right)^{d} Bo^{e}. \tag{7}$$

The empirical parameters A, b, c, d, e are given in Table 4.

The negative signs for coefficients b, c and positive for d, e are in accordance with the observed trends for bubble sizes and lifetimes with change in heat flux (Ja), subcooling, flow rates (Bo) and pressure.

The accuracy of presented correlations is satisfactory, with coefficients of correlation between 0.86 and 0.92 and coefficients of determination of about 0.75–0.8. The correlation for the maximum bubble diameters, and bubble growth times are shown in Figs. 9 and 10. Few points (large diameters) on these figures that are not well represented by the correlations correspond to the low heat flux region. Experimental data from the isolated bubble region are, generally, very well represented by given correlations.

6. Summary and conclusions

The experiments were carried out at pressures of 2 and 3 bar, in addition to already existing experiments at 1.05 bar, in order to cover systematically the boiling region from ONB to OSV.

Three different bubble behaviors have been distinguished as follows:

(1) *Low heat flux region*: Characterized by low bubble population. Nearly spherical bubbles slide long distances without changing significantly in size and shape, occasionally detaching from the surface and typically reattaching soon after.

(2) *Isolated bubble region*: Covering the major part between ONB and OSV. Bubbles are flattened after inception, becoming more elongated as they grow. The transition from flat to elon-

gated shape occurs near the maximum diameter. Bubbles typically slide a distance of a couple of diameters, detach from the surface and travel in the direction normal to the heater into the liquid core, where they collapse rapidly. The ejection diameters are smaller than maximum diameters, indicating significant condensation rates while bubbles are still attached to the wall. At ejection, bubbles are typically elongated in the direction normal to the surface of the heater.

(3) *Region of significant bubble coalescence*: Characterized by large bubbles with varying sizes and shapes. These bubbles are typically products of bubble coalescence and have different dynamics than bubbles in the isolated region. They were observed before the OSV, more pronounced at higher pressures particularly at low flow rates.

The transition between the low heat flux region and the isolated bubble region seems to happen abruptly leading to a change in the heat transfer mode. It is possible that this transition coincides with the transition from partial to fully developed boiling although this cannot be confirmed at this point.

The transition between the isolated bubble region and the region of significant bubble coalescence is smooth and related to increasing nucleation sites with increasing heat flux.

- Bubble size and lifetime generally decrease with increasing heat flux and bulk liquid velocity. The effect of the heat flux and flow rate on bubble diameters and life span is greater at lower heat transfer rates. At higher heat fluxes the change of the bubble size becomes less obvious.
- The effect of the moderate (10–30 K) subcooling and pressure (in the low pressure range: 1–3 bar) on bubble size and lifetime was also investigated. Bubble size and life span decrease with increasing subcooling or pressure. The results are in accordance with most of the previous experimental studies.
- New correlations for the maximum diameter, detachment diameter, bubble growth and condensation time and bubble lifetime have been proposed.

Experimental data from this study were used to develop semi-empirical correlations for determining the variation of bubble size and lifetime with the above mentioned variables. Dimensionless numbers, such as the Boiling number, Jakob number and dimensionless subcooling are used to correlate the data. The pressure dependence has been accounted for by the density ratio. The coefficients of correlation between 0.86 and 0.92 indicate satisfactory agreement between experimental data and proposed correlations for given experimental conditions.

- The bubble growth rates have been successfully correlated using the model of Akiyama and Tachibana (1974) with slightly modified constants.
- Observed and measured normal detachment diameters have been compared with several models, including Zuber (1961), Mikic et al. (1970), Zeitoun and Shoukri (1996), Serizawa (1979) and Unal (1976). Good agreement with the Unal's model has been noticed, indicating the importance of the microlayer evaporation during bubble growth.

References

Abdelmessih, A.H., Hooper, F.C., Nangia, S., 1972. Flow effects on bubble growth and collapse in surface boiling. Int. J. Heat Mass Transfer 15, 115–125.

Akiyama, M., Tachibana, F., 1974. Motion of vapor bubbles in subcooled heated channel. Bull. J.S.M.E. 17, 241–247.

Bibeau, E.L., 1993. Void growth in subcooled flow boiling for circular and finned geometries for low values of pressure and velocity. Ph.D. Thesis, Department of Mechanical Engineering, University of British Columbia.

Bibeau, E.L., Salcudean, M., 1994. A study of bubble ebullition in forced-convective subcooled nucleate boiling at low pressure. Int. J. Heat Mass Transfer 37, 2245–2259.

Bibeau, E.L., Salcudean, M., 1993. Subcooled void growth for finned and circular annular geometries at low pressures and low velocities. In: Proceedings of the 3rd World Conference on Exp. Heat Transfer, Fluid Mechanics and Thermodynamics, vol. 2, pp. 1183–1190.

Butterworth, D., Shock, R.A.W., 1982. Flow boiling. In: 7th International Heat Transfer Conference, vol. 1, paper RK15, pp. 11–30.

Cooper, M.G., Mori, K., Stone, C.R., 1983. Behaviour of vapor bubbles growing at a wall with forced flow. Int. J. Heat Mass Transfer 26, 1489–1707.

Del Valle, V.H., Kenning, D.B.R., 1985. Subcooled flow boiling at high heat flux. Int. J. Heat Mass Transfer 28, 1907–1920.

Faraji, D., Barnea, Y., Salcudean, M., 1994. Visualization study of vapor bubbles in convective subcooled boiling of water at atmospheric pressure. In: 10th International Heat Transfer Conference, paper 18-FB-4, pp. 425–430.

Frost, W., Kippenhan, C.J., 1967. Bubble growth and heat transfer mechanisms in the forced convection boiling of water containing a surface active agent. Int. J. Heat Mass Transfer 10, 931–949.

Gunther, F.C., 1951. Photographic study of surface boiling heat transfer to water with forced convection. Trans. ASME 73, 115–124.

Hahne, E., Spindler, K., Shen, N., 1990. Incipience of flow boiling in subcooled well wetting fluids. In: Proceedings of the 9th International Heat Transfer Conference, vol. 2, pp. 69–74.

Kandlikar, S.G., Mizo, V.R., Cartwright, M.D., 1995. Investigation of bubble departure mechanism on subcooled flow boiling of water using high speed photography. In: Proceedings of the Conference on Convective Flow Boiling, pp. 161–166.

Kandlikar, S.G., Stumm, B.J., 1995. A control volume approach for investigating forces on a departing bubble under subcooled flow boiling. Trans. ASME, J. Heat Transfer 117, 990–997.

Klausner, J.F., Mei, R., Bernhard, D.M., Zeng, L.Z., 1993. Vapor bubble departure in forced convection boiling. Int. J. Heat Mass Transfer 36, 651–662.

Koumoutsos, N., Moissis, R., Spyridonos, A., 1968. A study of bubble departure in forced convection boiling. Trans. ASME, J. Heat Transfer 90, 223–230.

Mikic, B.B., Rohsenov, W.M., Griffith, P., 1970. On bubble growth rates. Int. J. Heat Mass Transfer 13, 657–665.

Roy, R.P., Velidandla, V., Kalra, S.P., Peturaud, P., 1994. Local measurements in the two-phase region of turbulent subcooled boiling flow. Trans. ASME, J. Heat Transfer 116, 660–669.

Serizawa, A., 1979. A study of forced convection subcooled flow boiling. In: Drust, F., Tsiklauri, G.V., Afgan, N.H. (Eds.), Two-Phase Momentum, Heat and Mass Transfer in Chemical Processes and Energy Engineering Systems, vol. 1, pp. 231–242.

Thorncroft, G.E., Klausner, J.F., Mei, R., 1998. An experimental investigation of bubble growth and detachment in vertical upflow and downflow boiling. Int. J. Heat Mass Transfer 41, 3857–3871.

Tolubinsky, V.I., Kostanchuk, D.M., 1970. Vapour bubbles growth rate and heat transfer intensity at subcooled water boiling. In: 4th International Heat Transfer Conference, vol. 5, paper B2.8.

Unal, H.C., 1976. Maximum bubble diameter, maximum bubble-growth time and bubble-growth rate during the subcooled nucleate flow boiling of water up to 17.7 MN/m^2. Int. J. Heat Mass Transfer 19, 643–649.

Zeitoun, O., Shoukri, M., 1996. Bubble behavior and mean diameter in subcooled flow boiling. Trans. ASME, J. Heat Transfer 118, 110–116.

Zeng, L.Z., Klausner, J.F., Bernhard, D.M., Mei, R., 1993. A unified model for the prediction of bubble detachment diameters in boiling systems – II. Flow boiling. Int. J. Heat Mass Transfer 36, 2271–2279.

Zuber, N., 1961. The dynamics of vapor bubbles in nonuniform temperature fields. Int. J. Heat Mass Transfer 2, 83–98.